Antiferromagnetic-ferromagnetic transition in FeRh

V. L. Moruzzi and P. M. Marcus

IBM Research Division, Thomas J. Watson Research Center, P.O. Box 218, Yorktown Heights, New York 10598

(Received 6 February 1992)

First-principles band-structure calculations based on the augmented-spherical-wave method and the fixed-spin-moment procedure are used to determine the volume dependence of the total energy and the local moments in ordered FeRh. The calculations reveal the coexistence of antiferromagnetic (AF) and ferromagnetic (FM) solutions over a wide range of volume. The zero-pressure equilibrium state is found to be AF with $\sim \pm 3.0 \mu_B$ iron local moments and precisely zero rhodium local moments, in agreement with experiment, and the calculated lattice constant is within 0.14% of the experimental value. A metastable ferromagnetic state with iron and rhodium local moments of $\sim 3.1 \mu_B$ and $1.0 \mu_B$ lies just above the AF state and has a minimum energy at a lattice constant $\sim 0.5\%$ larger than the AF state, implying that when the system undergoes the AF-FM transition at finite temperatures, the transition is accompanied by an enhanced thermal expansion. At expanded volumes, the FM state becomes energetically more favorable than the AF state. Calculations also show that type-II AF is more stable than type-I AF in the CsCl structure, in agreement with experiment.

I. INTRODUCTION

FeRh in the ordered CsCl structure, which was found to undergo a transition from antiferromagnetic (AF) to ferromagnetic (FM) behavior by heating above room temperature by Fallot and Hocart[1] over 50 years ago, has been intensively studied both experimentally and theoretically. At low temperatures, experiment shows that FeRh is AF with iron local moments of $\sim \pm 3 \mu_B$ with no appreciable rhodium moments. At high temperatures, the system is found to be FM with iron and rhodium local moments of ~ 3 and $1 \mu_B$, respectively. The transition occurs at a temperature $T_{tr} \sim 340$ K with no change in the CsCl structure.[2] At T_{tr}, the thermal expansion undergoes[3] an abrupt "enhancement," which is manifested by an $\sim 0.3\%$ lattice expansion. The transition from ferromagnetic to paramagnetic behavior occurs[3,4] at a Curie temperature, $T_{Curie} \sim 670$ K. No Néel temperature is detected. In addition, it is found[3] that the AF-FM transition can be induced by a critical magnetic field H_{cr} which varies with temperature and which goes to zero at T_{tr}. Under the influence of pressure, T_{tr} increases.[5] Above T_{tr}, positive pressures again stabilize[6] the AF state by inducing the inverse FM-AF transition. These unusual properties are very sensitive to stoichiometry. It is observed that a few percent increase[7] in the iron content causes a substantial decrease in T_{tr} and that the critical fields necessary to induce the transition can vary by almost a factor of 2 for different alloys near the stoichiometric composition.[3]

In 1960, Kittel[8] suggested that AF-FM transitions can be due to a volume-dependent exchange inversion. In this model, a system is decomposed into two identical sublattices which are coupled by an exchange interaction that changes sign at a critical lattice constant. Thermal expansion through this critical lattice constant was proposed as a possible explanation of the AF-FM transition.

However, Kouvel[9] noted an anomalously large increase in the magnetic entropy at the transition temperature and observed that this was incompatible with an exchange inversion model. Tu *et al.*[10] proposed that this excess magnetic entropy actually stabilizes the FM state. Attempts to understand the properties of the FeRh system in terms of exchange inversion and/or stabilizing magnetic entropy do not provide a reliable description of the transition.

Although it has long been recognized that first-principles band-structure calculations may be useful for studying the AF-FM transition in ordered FeRh, existing calculations fall short of this goal. Early calculations are either non-self-consistent[11] or non-spin-polarized[5,11] and are therefore incapable of addressing magnetic implications. More recent[12] band-structure calculations, based on the linear muffin-tin orbital (LMTO) method, the atomic-sphere approximation (ASA), and the local-density approximation (LDA) to density-functional theory, explicitly consider the nonmagnetic, ferromagnetic and antiferromagnetic forms of ordered FeRh. These latter calculations, however, are all done for the experimental lattice constant and do not attempt to study the relative stabilities of the AF and FM states by total-energy comparisons. Hasegawa[13] attempted to study this relative stability by using a canonical *d*-band model and the Hartree-Fock and coherent-potential approximations. These calculations involve a number of adjustable parameters which are determined from experimental properties. Although useful, these are not first-principles calculations, and they do not prove that the equilibrium state is AF or show that the AF-FM transition must occur.

The present work makes use of extensive calculations of the volume dependence of the total energies and of the local magnetic moments of iron and rhodium. The results show that the equilibrium state is type-II AF with large iron local moments and zero rhodium local moments; that a metastable FM state exists a few mRy

above the AF state and with an $\sim 0.5\%$ larger lattice constant, and make plausible that an AF-FM transition at finite temperature would be accompanied by an abrupt expansion to a larger lattice constant. The present work provides an example of a first-principles electronic structure calculation that shows unambiguously that the equilibrium state of a transition-metal element or alloy is antiferromagnetic, and shows that FeRh is an example of anti-Invar,[14] a transition-metal system which exhibits "enhanced" rather than "invariant" thermal expansion.

This work represents a substantial extension of our previous work on magnetic properties of transition-metal elements using constrained total-energy calculations. Studies of the elements in cubic structures in the FM state can be made with one-atom cell calculations and in the AF state can be made with two-atom cell calculations. For binary compounds like FeV or FeRh with the CsCl structure, two-atom cells are required to study FM, four-atom cells are required to study type-I and type-II AF. The fixed-spin-moment constraint then becomes even more important for separating the many magnetic solutions of the spin-polarized Kohn-Sham equations of the system with the many degrees of freedom implicit in the larger magnetic unit cells.

II. BAND CALCULATIONS

The spin configurations for type-I and II antiferromagnetism for the CsCl unit cell of FeRh are shown in Fig. 1. The antiferromagnetic coupling for type-I AF is between successive layers of (001) iron planes, while for

type-II AF it is between successive layers of (111) iron planes.[15] The experimentally determined configuration is type-II AF. The tetragonal magnetic unit cell used in our calculations to capture both observed FM and type-II AF (as well as nonmagnetic) states is shown in Fig. 2. Here, the lattice constant $a = \sqrt{2}a^*$, where a^* is the basic CsCl lattice constant, and $c = \sqrt{2}a$. The unit cell contains a total of eight atoms and consists of alternate layers of iron and rhodium atoms with two inequivalent atoms in each layer. Supplementary calculations using a four-atom magnetic unit cell consisting of a double stack of the cell shown in Fig. 1 (I) were done in order to study the relative stability of type-I and -II antiferromagnetism. The eight-atom type-II AF cell was chosen over the equivalent four-atom fcc cell to insure similar Brillouin-zone $\mathbf{k}$ sampling.

Our total-energy band-structure calculations are based on the augmented-spherical-wave (ASW) method of Williams, Kübler, and Gelatt,[16] which uses the atomic-sphere approximation with sphericalized potentials within Wigner-Seitz spheres of radius r_{WS}, and the local-density approximation as formulated by von Barth and Hedin and modified by Janak[17] to account for exchange and correlation. Our calculations also utilize a fixed-spin-moment (FSM) procedure which, for fixed volumes V, allows us to determine total energies as a function of constrained values of the total magnetic moment M of the assumed magnetic unit cell. Minima in resulting $E(M)_V$ curves give solutions that are stable in zero applied field (zero-field solutions) and also give the corresponding total energies and local magnetic moments. The calculations are nonrelativistic, assume collinear spins, and are done on a uniform mesh of 40 $\mathbf{k}$ points in the irreducible part of the first Brillouin zone.

The ASA approximation with Wigner-Seitz spheres used in our work requires that the volume V of the unit cell be assigned to constituent atomic spheres with radii
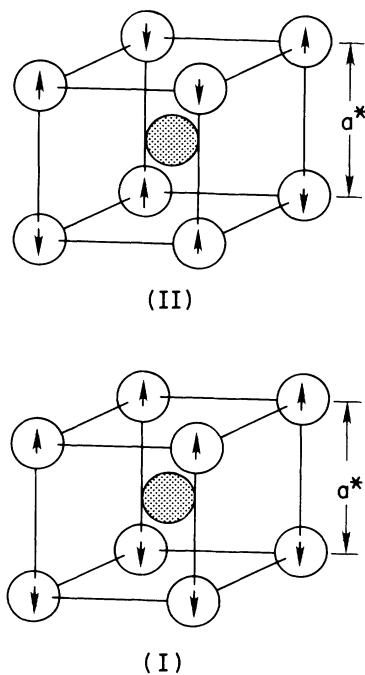

(II)

(I)

FIG. 1. Spin configurations for type-I and type-II antiferromagnetism for the basic CsCl unit cell for FeRh. Shaded and open spheres represent rhodium and iron atoms. Configuration (II) with no spin on the rhodium atom is experimentally observed. In the ferromagnetic state, all iron and rhodium spins are parallel.
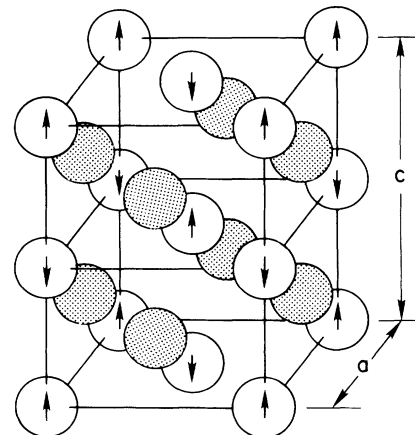

FIG. 2. Magnetic unit cell used to study both antiferromagnetic and ferromagnetic states in FeRh. Shaded and open spheres represent rhodium and iron atoms, respectively. Arrows indicate the antiferromagnetic iron spin configuration. In the antiferromagnetic state, the rhodium atoms have no local moments. In the ferromagnetic state, all iron spins and rhodium spins are parallel.

r_{Fe} and r_{Rh} such that the sum of the sphere volumes is V. In this work, we arbitrarily chose the two sphere radii to be equal to a Wigner-Seitz radius, r_{WS}. For type-II AF,

$$V = 8(4\pi/3)r_{WS}^3 = a^3(c/a).$$

III. RIGID-LATTICE RESULTS

In the FSM procedure used in all of our band-structure calculations, we determine the total energy E of a system constrained to have a given magnetic moment M per unit cell. At a given volume, the constrained moment M is varied to find $E(M)$. The advantage of this procedure over conventional "floating-moment" spin-polarized calculations is that the constraint restricts fluctuations in the self-consistent procedure, which can delay the convergence and make the results uncertain. In addition, by varying the moment we find all solutions (nonmagnetic, ferromagnetic, and antiferromagnetic) to the band equations.

A. Total energies and local moments versus total moment

Typical calculated total energies and local moments as a function of M for FeRh are shown in Figs. 3–6 for volumes corresponding to r_{WS} values ranging from below equilibrium to above the AF-FM transition. We note that, although we considered the eight-atom magnetic unit cell to have two inequivalent iron and two inequivalent rhodium atoms, the rhodium atoms have equal
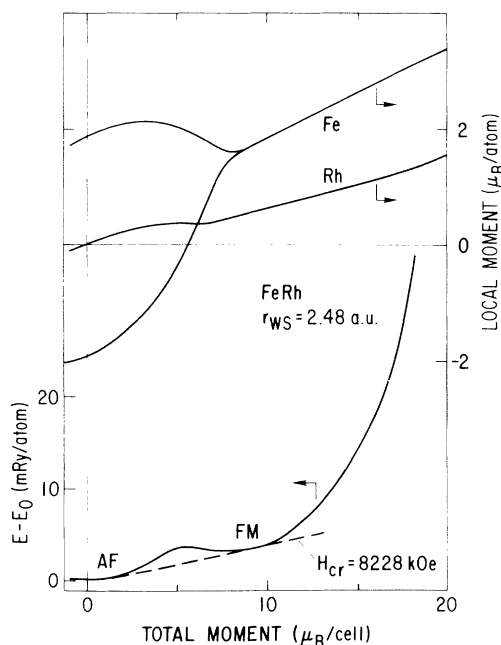

FIG. 4. Total energy vs constrained magnetic moment for FeRh at $r_{WS} = 2.66$ a.u. showing the AF and FM stable solutions. E_0 is the minimum energy for this r_{WS} value.

moments at all values of the constrained total moment, M. This result can be considered to be a calculational verification of the results obtained by Hargitai[18] that a combination of Landau theory and group theory requires zero local moments for the rhodium atoms in the AF

FIG. 3. Total energy vs constrained magnetic moment for FeRh at $r_{WS} = 2.48$ a.u. E_0 is the minimum energy for this r_{WS} value. This volume marks the lower end of the stability region for the FM solution. The AF and FM states are in equilibrium at the external field represented by the indicated common-tangent construction. In the FM region and at this volume, the rate of increase of the iron local moment is greater than that of the rhodium local moment.
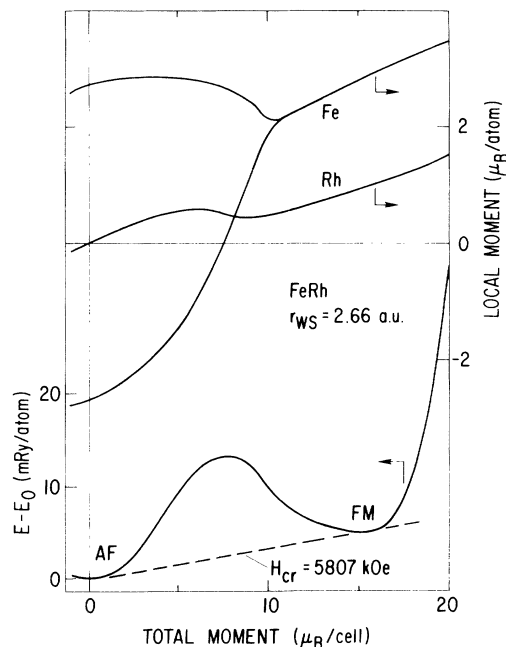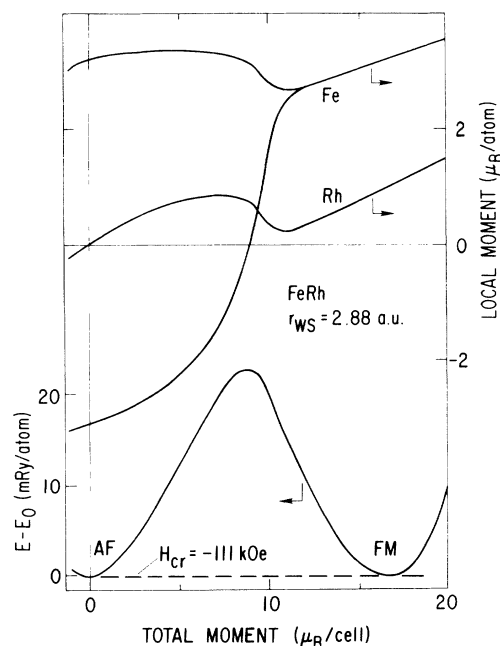

FIG. 5. Total energy vs constrained magnetic moment for FeRh at $r_{WS} = 2.88$ a.u. E_0 is the minimum energy for this r_{WS} value. Here the critical field becomes negative. In the FM region and at this volume, the rate of increase of the iron local moment is less than that of the rhodium local moment.
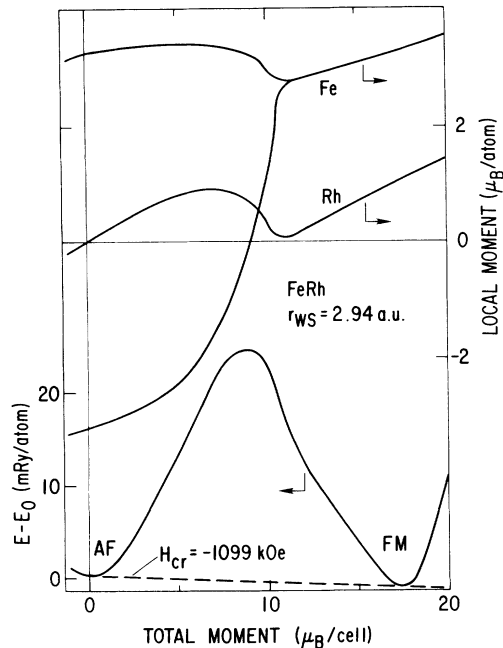
ANTIFERROMAGNETIC-FERROMAGNETIC TRANSITION IN FeRh

FIG. 6. Total energy vs constrained magnetic moment for FeRh at $r_{WS} = 2.94$ a.u. E_0 is the minimum energy for this r_{WS} value.

state. In fact, our results go further and show that the rhodium local moments are equal for all values of constrained total moment, even when they acquire nonzero local values. Accordingly, the rhodium atoms were all constrained to be equivalent in most of the calculations. A simple symmetry argument can be given for this equivalence of the rhodium local moments. The two rhodium atoms have equivalent, although spatially inverted, physical surroundings (Fig. 2) for all values of total moment M. Since the iron atoms are AF at $M = 0$, the rhodium atoms must both have zero moment.

A variety of magnetic properties can be obtained from the calculated local magnetic moment and energy curves as functions of M. The minima in the $E(M)$ curves correspond to stable (or metastable) AF and FM states of the system; the minima at $M = 0$ correspond to stable (or metastable) AF solutions where the rhodium atoms have zero local moments and the two inequivalent iron atoms have large equal and opposite local moments. As M increases, the spin-down iron moments generally decrease in magnitude, go through zero, and approach the spin-up iron moments. Simultaneously, the rhodium atoms acquire a moment which generally increases. The $E(M)$ curves display a local maximum at about the moment where the two iron local moments merge. In this region, the rhodium and the spin-up iron local moments exhibit a dip before assuming a rather linear increase. The minima at large values of total moment correspond to stable (or metastable) FM solutions with spin-up local moments on both rhodium and iron atoms.

With increasing r_{WS}, the energy "barrier" between the AF and FM solutions increases, but the energy difference between the minima, $E_{FM} - E_{AF}$, decreases and changes sign at $r_{WS} \sim 2.88$ a.u., where the FM state becomes more

favorable. We note that, at large M, the rate of increase of the local iron moment is greater than that of the local rhodium moment for low r_{WS} values and lower for large r_{WS} values.

By symmetry the total energy for negative total moments must be the same as for positive total moments. However, the local moments will change sign. The symmetric $E(M)$ and antisymmetric local-moment curves for $r_{WS} = 2.40$ a.u. are shown in Fig. 7. For this volume, there is no FM solution. In fact, the AF solution is just barely stable; the local AF iron moments are only $\sim \pm 1 \mu_B$. At $r_{WS} = 2.30$ a.u., the solution for $M = 0$ is nonmagnetic (all local moments are zero). At this lower volume, the hysteresis-like local iron moment loop shown in Fig. 7 collapses and both the iron and rhodium local moments vary linearly with the total moment.

At volumes where there are both stable AF solutions and metastable FM solutions, an external field can bring the two states into thermodynamic equilibrium. This external field can be determined by the common-tangent construction shown in Figs. 3–6. At the indicated volume-dependent critical field H_{cr} the AF and FM states are in equilibrium. This is the magnetic analog of the critical pressure obtained by the common-tangent construction applied to different branches on $E(V)$ graphs.[14] With increasing volume, H_{cr} decreases, goes through zero, and becomes negative at volumes which favor the FM solution. Although the calculated critical fields are larger than observed,[3] a similar construction between free-energy curves at finite temperatures is expected to yield the experimental critical fields. Negative fields correspond to fields directed antiparallel to the ferromagnetic spins.

In Table I, we summarize the results of our $E(M)$ and local-moment calculations for different r_{WS} values. Listed are (1) the energy difference between the FM and AF minima of the $E(M)$ curves, (2) the average magnetic moment at the FM minimum, (3) the calculated critical field, (4) the iron local moments for the AF minimum (where
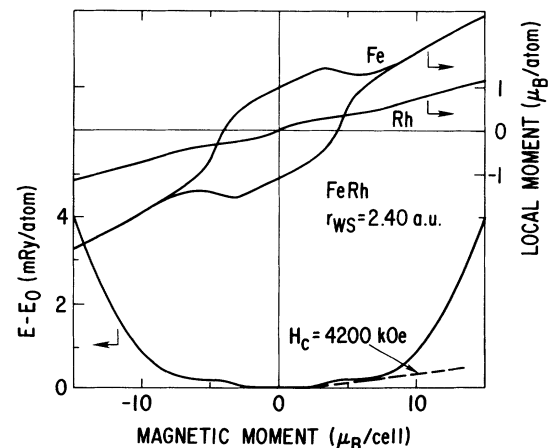

FIG. 7. Total energy vs constrained positive and negative magnetic moment for FeRh at $r_{WS} = 2.40$ a.u. E_0 is the minimum energy for this r_{WS} value.

TABLE I. Calculated ferromagnetic and antiferromagnetic quantities vs Wigner-Seitz radii r_{WS} for FeRh. NA signifies "not applicable." At $r_{WS} = 2.30$ a.u., the system is nonmagnetic and there are no AF or FM local moments.

r_{WS} (a.u.)	$E_{FM} - E_{AF}$ (mRy/atom)	M_{FM} (μ_B/atom)	H_{cr} (kOe)	$m_{Fe}(AF)$ (μ_B/atom)	$m_{Fe}(FM)$ (μ_B/atom)	$m_{Rh}(FM)$ (μ_B/atom)
2.30	NA	NA	NA	0.00	0.00	0.00
2.36	NA	NA	NA	0.20	0.00	0.00
2.38	NA	NA	2820	0.30	0.00	0.00
2.40	NA	NA	4200	0.95	0.00	0.00
2.48	3.25	1.00	8800	1.87	1.54	0.46
2.54	5.50	1.25	9990	2.26	1.91	0.59
2.60	6.25	1.62	8934	2.52	2.45	0.80
2.66	5.00	1.87	6286	2.74	2.82	0.98
2.70	4.00	2.00	4702	2.82	2.98	1.02
2.72	3.50	2.04	4034	2.86	3.06	1.02
2.74	3.00	2.06	3422	2.92	3.10	1.02
2.76	2.50	2.07	2838	2.93	3.12	1.02
2.78	2.12	2.07	2407	2.98	3.12	1.02
2.80	1.75	2.08	1977	3.04	3.15	1.02
2.82	1.25	2.10	1399	3.06	3.18	1.02
2.84	0.75	2.10	839	3.09	3.18	1.02
2.86	0.37	2.11	412	3.14	3.19	1.02
2.88	−0.10	2.11	−111	3.18	3.20	1.02
2.90	−0.37	2.13	−408	3.20	3.23	1.02
2.94	−1.00	2.14	−1099	3.24	3.26	1.02
3.00	−1.63	2.18	−1763	3.30	3.32	1.04

the rhodium local moments are zero), and (5) the iron and rhodium local moments at the FM minimum. As shown in Table I and as Fig. 3 implies, we lose the FM minimum somewhere between $r_{WS} = 2.48$ and 2.40 a.u. That is, the zero-field FM solutions terminate at $r_{WS} \sim 2.48$ a.u. Note that, because of residual FM influence, common-tangent constructions and the associated critical fields persist even at volumes where there are no FM minima. Over 1000 fully self-consistent band-structure calculations (approximately 50 for each r_{WS} value) were required to obtain the data listed in Table I.

B. Total energies and local moments versus volume

The local minima corresponding to $dE/dM = 0$ in our calculated $E(M)$ curves correspond to zero-field rigid-lattice solutions. The energies corresponding to these solutions, as functions of r_{WS} near the equilibrium volume, are shown in Fig. 8. Note that there are two distinct branches, one for the AF and one for the FM solutions. Moreover, note that the AF branch has a lower minimum than the FM branch, implying that the rigid-lattice ground state is AF, as is experimentally observed. The equilibrium volume, given by the minimum of the AF branch, corresponds to $r_{WS} = 2.782$ a.u. This compares favorably with the value $r_{WS} = 2.778$ a.u. obtained from the experimental lattice constant given by Shirane, Nathans, and Chen.[19] At expanded volumes, the FM state becomes more stable.

Different bulk moduli, Grüneisen constants, and Debye temperatures are associated with the two branches of the binding curves shown in Fig. 8. In order to evaluate

these quantities, we first fit the calculated points to the four-parameter Morse function

$$E(r_{WS}) = A - 2De^{-\lambda(r_{WS}-r_0)} + De^{-2\lambda(r_{WS}-r_0)},$$

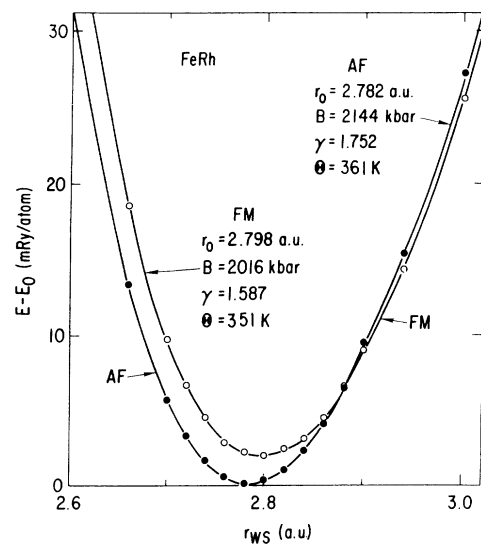where r_0 is the equilibrium Wigner-Seitz radius. The pa-

FIG. 8. Zero-field total energy vs r_{WS} for the FeRh rigid lattice near the equilibrium volume. E_0 is the minimum energy for the AF state. The points are derived from $E(M)$ curves like those of Figs. 3-7. Solid points are AF solutions and open points are FM solutions. The lines are derived from the Morse parameters listed in Table II.

TABLE II. Morse parameters, bulk moduli B, Grüneisen constants γ, and Debye temperatures Θ for the rigid-lattice AF and FM branches of the $E(r_{WS})$ curves for FeRh shown in Fig. 8. The linear parameters D and A are in Ry/atom and B is in kbar.

Branch	r_0 (a.u.)	λ (a.u.$^{-1}$)	D	A	B	γ	Θ (K)
AF	2.782	1.2595	0.4819	-5944.3676	2144	1.752	361
FM	2.798	1.1342	0.5616	-5944.2860	2016	1.587	351

rameters, r_0, λ, D, and A, resulting from a least-squares fit and the bulk moduli B, Grüneisen constants γ, and Debye temperatures Θ derived[20] from the fit are listed in Table II.

The local moments associated with the AF and FM branches of Fig. 8 are shown in Fig. 9. At the equilibrium volume the local iron moments, although nearly equal, are slightly lower for the AF than for the FM state. Neutron-diffraction studies[19] reach the opposite conclusion. The FM local moments terminate at $r_{WS} = 2.48$ a.u. The local iron AF moments extend to lower r_{WS} values and appear to approach zero (i.e., become nonmagnetic) smoothly, displaying no discontinuity in slope. Our past experiences with simpler systems suggest that this smooth approach to zero moment is not valid. We attribute this behavior to an averaging of nonmagnetic and nearby (in volume) AF solutions, and believe that the "correct" form should be singular, as was shown[21] for magnetovolume transitions from nonmagnetic to ferromagnetic behavior. That is, the AF local iron moments should approach zero with infinite slope at some critical volume (or at a critical r_{WS} value). We estimate this critical point to be at $r_{WS} \sim 2.38$ a.u.
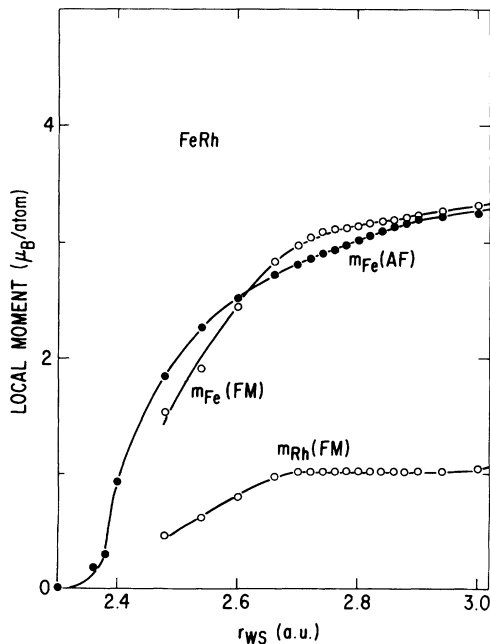
From Table I, we see that, for the FM state and for

$r_{WS} > 2.68$ a.u., the rhodium local moment assumes a constant value of $1.02\mu_B$, a value consistent with the Hund's-rule free-atom value. Note that this moment corresponds only to the stable FM state and that it can be increased (decreased) by increasing (decreasing) the constrained value of the total moment.

In Fig. 10, we show the energy difference, $E_{FM} - E_{AF}$, vs r_{WS}. Below $r_{WS} = 2.48$ a.u., this curve is nonexistent because of the termination of zero-field FM solutions. With increasing r_{WS}, this energy difference first increases, goes through a peak near $r_{WS} \sim 2.6$ a.u., and then decrease monotonically, going through zero at $r_{WS} \sim 2.87$ a.u. (where the AF and FM branches cross, as shown in Fig. 8). The initial increase in this energy difference is a consequence of the large rate of change of the FM moment in this volume range. In Fig. 10, we also show the related function, $H_{cr}(r_{WS})$. Note that we can extend H_{cr} to lower r_{WS} values than the energy difference since there is still a bulge in the FM energy curve even when the minimum is gone (see Fig. 7).

The $E(M)$ curves shown in Figs. 3–7 (and 12) all assume that the spins are collinear. The FSM procedure used here corresponds to doing band-structure calcula-

FIG. 9. Local moments for AF (solid points) and FM (open points) zero-field solutions for the FeRh rigid lattice.
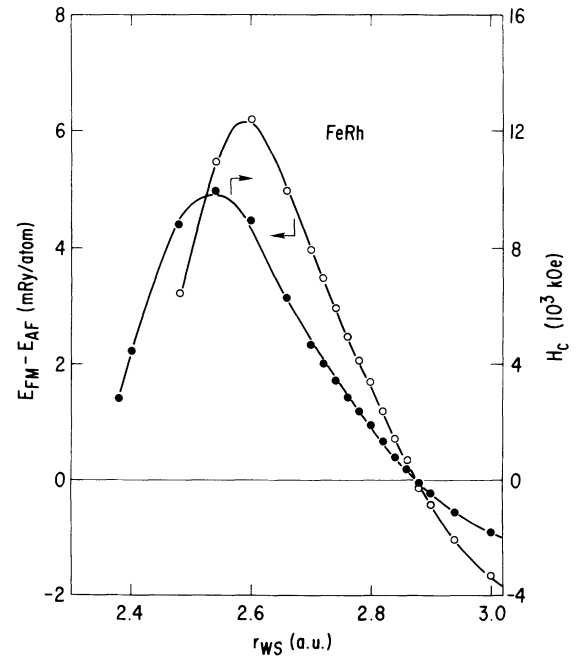
FIG. 10. Critical rigid-lattice magnetic fields (solid points) and energy difference between the AF and FM solutions (open points).

tions with the system in an effective external magnetic field given by dE/dM. For an antiferromagnetic system, even in a relatively low field, spins antiparallel to the field will tend to bend into the field direction, resulting in non-collinear local moments if the vector character is introduced. Therefore, the collinear spin arrangements and total energies implied in our $E(M)$ curves for the AF states as M increases from zero are unrealistic. However, at $dE/dM = 0$, the field vanishes and our collinear assumption is expected to hold. Therefore, our results for the AF and FM minima and the implied critical fields are expected to be valid.

As mentioned above, the results in Table I are derived from over 1000 band-structure calculations done over a range of values of r_{WS} and total moment. Each calculation is self-consistent and includes the determination of energy bands and density of states (DOS). In Fig. 11, we show the local DOS for iron and rhodium for our type-II AF calculation $(M = 0)$ and our FM calculation $(M = 16.5\mu_B)$ for FeRh at $r_{WS} = 2.80$ a.u. Our results show that the iron moment is strongly enhanced (compared to the elemental bcc iron moment) by a complete filling of the up-spin bands and by the associated decrease in occupation of the down-spin bands for both the AF and FM states. In fact, the shapes of the bands differ substantially from the bcc iron bands[22] with much of the weight shifted to lower energies for the up-spin bands and to higher energies for the down-spin bands, which now have a large peak above the Fermi energy.

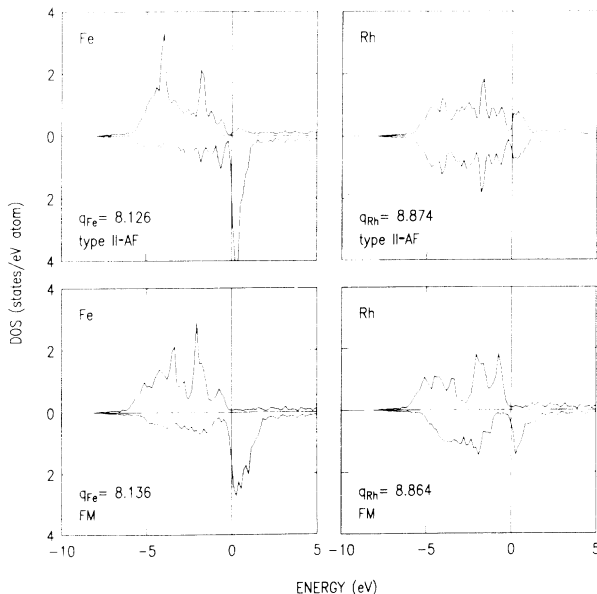In addition to these differences in the iron AF and FM

FIG. 11. Local density of states (DOS) for iron (left panels) and rhodium (right panels) in the type-II AF (upper panels) and the FM (lower panels) states for FeRh at $r_{WS} = 2.80$ a.u. The up-spin DOS is shown above and the down-spin DOS is shown below the zero DOS line. q is the charge associated with each atom. The spin-up and spin-down charges can be obtained from Table I, which lists the local magnetic moments, or the differences in charges.

bands, there are significant differences in the rhodium AF and FM bands. In the AF state, the up-spin and down-spin rhodium bands are identical, reflecting the fact that the local rhodium moment is zero. In the FM state, the rhodium up-spin and down-spin bands are split, resulting in a rhodium local moment of about $1\mu_B$.

Although the AF and FM DOS differ in detail, we find a similar charge transfer of about 0.13 electrons from rhodium to iron (normally, iron has eight and rhodium has nine valence electrons) in both cases. The DOS for iron at the Fermi energy is also almost identical for the AF and FM states, amounting to 0.08 and 1.71 states/eV atom for the up-spin and down-spin bands, respectively. This similarity in values between the AF and FM iron DOS contrasts with the results of Koenig[12] who finds 0.44 and 2.58 states/eV atom for the iron up-spin and down-spin bands, respectively, for the AF state, and 0.06 and 0.73 states/eV atom for the FM state.

We can also compare our total DOS at the Fermi energy with the calculation of Koenig[12] and the low-temperature specific-heat measurements of Tu et al.[10] Our values for the AF and FM states are, respectively, 2.75 and 2.34 states/eV for an FeRh formula unit, with the AF value slightly larger than the FM value. Koenig's results are 1.02 and 4.76 states/eV per formula unit, with the FM value a factor of 4 larger than the AF value. The experimental result[10] for $Fe_{0.49}Rh_{0.51}$, which is AF at low temperatures, is 1.08 states/eV, and for $Fe_{0.51}Rh_{0.49}$, which is FM at low temperatures, is 4.04 states/eV. Our result is approximately midway between the two measurements, as might be expected for a composition midway between these two stoichiometries. Hence, in contrast with Koenig, we interpret the experimental difference to be due to the difference in compositions rather than to a property of $Fe_{0.50}Rh_{0.50}$. The fact that our total DOS at the Fermi energy is not very different in the AF and FM states is consistent with the conclusions of Chen and Lynch[23] based on measurements of the dielectric function that the "band structure of FeRh is not drastically affected as the antiferromagnetic-ferromagnetic phase transition occurs."

C. Type-II vs type-I antiferromagnetism

The stability of type-II vs type-I antiferromagnetism for FeRh is implicit in Fig. 12, where we show the total energy versus constrained moment (μ_B/atom) for two FeRh calculations with the spin configurations shown in Fig. 1 for $r_{WS} = 2.80$ a.u., close to the equilibrium volume. At large values of the constrained moment, where all spins are parallel (i.e., where the solutions are ferromagnetic), the two calculations are identical and have identical $E(M)$ behavior (the type-I and type-II calculations have four and eight atoms per magnetic cell, respectively). The equivalence of the two $E(M)$ curves for $M > \sim 0.5\mu_B$/atom shows that the two sets of calculations are well converged and that the number of k points used is adequate. At $M = 0$, we see that the type-II AF solution is more stable than the type-I AF solution, in agreement with the experimental observation. The energy difference between type II and type I is 1.75
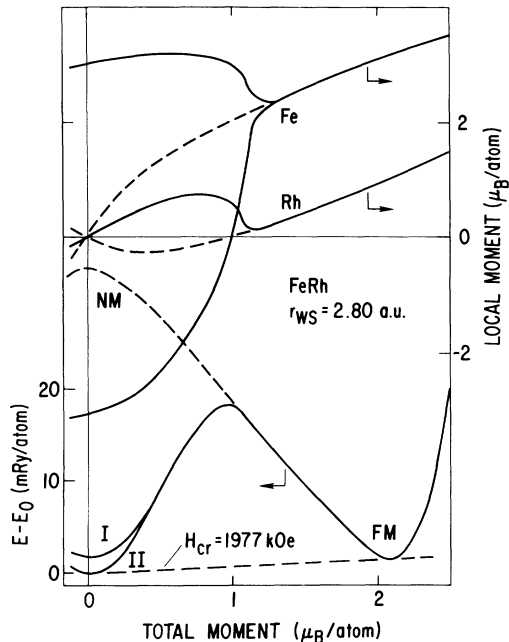
FIG. 12. Total energy vs constrained (average) moment for four- and eight-atom magnetic cells implied in Fig. 1 for $r_{WS} = 2.80$ a.u. and used to study the relative stability of type-I and type-II antiferromagnetism in FeRh. The dashed lines correspond to an unstable nonmagnetic (at $M = 0$) solution. E_0 is the minimum energy for this r_{WS} value. At $r_{WS} = 2.80$ a.u., type II is 1.75 mRy more stable than type I.

mRy/atom which corresponds to approximately 260 K. The iron local moments derived from the type-I and -II calculations are nearly identical, even at $M = 0$, where the energy difference is greatest. Another $E(M)$ branch, corresponding to an unstable nonmagnetic (NM) solution (dashed lines), is also found. The band equations have multiple solutions (i.e., type-I and -II AF, NM, and FM) that can be found by using different starting potentials in the iteration procedure used to achieve self-consistency. A qualitative argument that type-II AF is more stable than type-I AF in the simple-cubic iron lattice is made by observing that all near neighbors of a given iron atom have the opposite spin in type-II AF but have mixed spins in type-I AF.

Our result that type-II AF is more stable than type-I AF only applies to cubic structures. Since type-I AF breaks the cubic symmetry around each iron atom, a tetragonal distortion will lower the total energy. Evidently this lowering of the type-I AF total energy is not enough to reverse the order of stabilities since the experimental[19] structure is cubic and type-II AF.

IV. TEMPERATURE EFFECTS

The results presented above are all rigid-lattice rigid-spin results. Temperature-driven lattice vibrations and spin fluctuations are not included in the calculations. The results, in fact, do not even apply for zero temperature because zero-point lattice vibrations are also missing.

At finite temperatures, lattice vibrations and spin fluctuations contribute to the free energy and change the curves in Fig. 8. Using Debye-Grüesien theory to account for lattice vibrations in simple (nonmagnetic) metals leads to a shifting of the free energy to successively lower energies accompanied by a shift in the minimum to larger r_{WS} values due to the anharmonic character of the binding curves. This shift to larger r_{WS} values successfully explains the observed thermal expansion.[20] The same general behavior is expected for magnetic and antiferromagnetic systems. Thus, inclusion of the temperature dependency of the energy and entropy of lattice vibrations and spin fluctuations should shift the curves of Fig. 8 to lower energies and shift the positions of the two minima to successively larger r_{WS} values. Since the temperature-dependent energy and entropy of lattice vibrations and spin fluctuations is different for the AF and FM states, the two curves shift at different rates. In order to explain the observed AF-FM transition at $T_{tr} = 340$ K, the minimum of the FM free energy must fall below the minimum of the AF free energy. Hence, at T_{tr}, the AF-FM transition occurs and the system exhibits an abrupt expansion from the AF minimum to the larger FM minimum. It is plausible that this abrupt expansion should be approximately the same as the difference between the two minima depicted in the rigid-lattice total energy curves shown in Fig. 8, or approximately 0.5%. This theoretical value, derived from first-principles band-structure calculations with atomic numbers as the only input, may be compared with the experimentally determined value of 0.3%.

For all temperatures above T_{tr}, the minimum in the FM free-energy curve must be lower than that of the AF free-energy curve. As a consequence positive external pressures determined by the construction of a common tangent to the two (FM and AF) free-energy curves and similar to that used to determine H_{cr} yield critical pressures at which the two states are in thermal equilibrium. These pressures are temperature dependent and are expected to be zero at T_{tr} and to increase with increasing temperature.

A possible explanation of the anomalously large magnetic entropy at the transition found by Kouvel[9] is suggested by our calculations. We confirm by direct calculation that the rhodium moments in the AF state are locked in by symmetry to be precisely zero, whereas they have a finite variable moment in the FM state. Hence, the FM state has more magnetic degrees of freedom than the AF state and can be expected to have a larger magnetic entropy which will tend to stabilize the FM state. Since we also find at least three spin configurations with energies within a few mRy of each other at the equilibrium lattice constant (type-I and -II AF and FM), we expect large increases in magnetic entropy at temperatures which can excite these states, such as T_{tr}.

V. DISCUSSION

The FeRh results presented above bear an interesting relationship to results obtained[14,24] for the model Invar system, ordered Fe_3Ni. In both cases, the calculated

$E(r_{WS})$ curves must be represented by two separate branches associated with different magnetic states. For Invar, the two branches correspond to high-spin (HS) and low-spin (LS) ferromagnetic states, while for FeRh the two branches correspond to AF and FM states. In both cases, the two branches are separated by a few mRy/atom so that the metastable state is within thermal range of the stable rigid-lattice state. An important difference between the two systems is that for Invar the minimum for the more stable rigid-lattice HS state has a larger volume than the less stable LS state, while for FeRh the minimum for the more stable AF state has a smaller volume than the less stable FM state. This difference produces a pause in the thermal expansion for Invar, but an enhancement in the thermal expansion for FeRh. In both cases, the systems undergo a transition from one type of magnetic behavior to another. The Invar HS-LS transition is less obvious than the FeRh AF-FM transition because for Invar both states are ferromagnetic and the transition is less abrupt. In addition, the local moments for the FeRh system are appreciably larger than those of the Fe_3Ni system.

The two systems exhibit a large difference in the coexistence volume range of the two states. In Invar, the coexistence range of the HS and LS states is very narrow and only occurs at volumes below the equilibrium zero-pressure volume associated with the HS state. In FeRh, this coexistence extends over a large range and occurs at expanded as well as contracted volumes. Since the existence of critical field effects depends upon both states existing at the same volume, these effects have a much greater volume range, and are more observable in FeRh.

Another interesting comparison[25] is with FeV, which also exists in the ordered CsCl structure. However, FeV is FM in the ground state, and the equilibrium volume corresponds to $r_{WS} = 2.66$ a.u., which is considerably lower than that of FeRh. A striking difference between the two systems is that the local iron moment in FeV is

reduced to $\sim 1\mu_B$ at equilibrium, whereas it is enhanced to $\sim 3\mu_B$ in FeRh (in both the FM and AF states). A related difference is that the bulk modulus for FeV is greater than that of bcc Fe (or bcc V), whereas that of FeRh is less than that of bcc Fe. These differences are partially explained by the expansion of the lattice produced by the larger moments, which thereby reduce the bulk modulus (which is expected to fall rapidly with lattice expansion).

The results presented here illustrate the diverse effects that can occur in binary magnetic systems. With many more degrees of freedom than in the elements, many magnetic solutions can exist at a given volume. For FeRh, our calculations confirm the presence of an AF equilibrium state and the preference for type-II over type-I AF, and find a FM equilibrium state at slightly higher volume and energy which suggests the possibility of an AF-FM transition at finite temperature. Our calculations imply a pause in the thermal expansion for Invar as the system undergoes a transition from a larger volume HS state to a lower volume LS state, but an enhancement in the thermal expansion for FeRh as the system undergoes a transition from a lower volume AF state to a larger volume FM state. Thus, FeRh is an anti-Invar system in the sense discussed in Ref. 14.
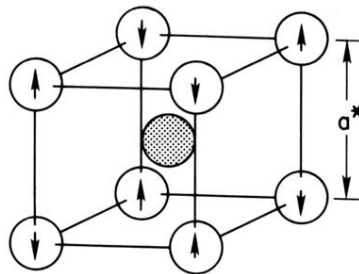
Finally, we comment that the reliability of our results, which are derived from first-principles calculations with atomic numbers as the only inputs, is supported by quantitative agreement with experiment of five ground-state properties, namely, the lattice constant and the local magnetic moments of the iron and rhodium atoms in both the AF and FM states.
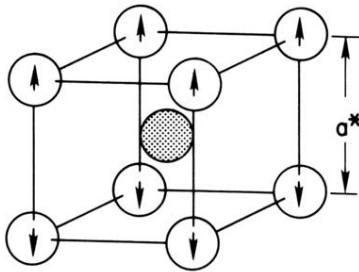
ACKNOWLEDGMENTS

[1] M. Fallot and R. Hocart, Rev. Sci. 77, 498 (1939).

[2] F. DeBergevin and L. Muldawer, C. R. Acad. Sci. 252, 1347 (1961).

[3] J. B. McKinnon, D. Melville, and E. W. Lee, J. Phys. C 1, S46 (1970).

[4] J. S. Kouvel and C. C. Hartelius, J. Appl. Phys. Suppl. 33, 1343 (1962).

[5] N. I. Kulikov, E. T. Kulatov, L. I. Vinokurova, and M. Pardavi-Horvath, J. Phys. F 12, L91 (1982).

[6] V. G. Veselago, L. I. Vinokurova, A. V. Vlasov, N. I. Kulikov, B. K. Ponomarev, M. Pardavi-Horvath, and L. I. Sagoyan, in The Magnetic and Electron Structure of Transition Metals and Alloys, edited by V. G. Veselago and L. I. Vinokurova (Nova Science, Commack, 1988), p. 45

[7] L. Pal, G. Zimmer, M. Pardavi-Horvath, and J. Paitz, J. Phys. (Paris) Colloq. 32, C-1-861 (1971).

[8] C. Kittel, Phys. Rev. 120, 335 (1960).

[9] J. S. Kouvel, J. Appl. Phys. 37, 1257 (1966).

[10] P. Tu, A. J. Heeger, J. S. Kouvel, and J. B. Comly, J. Appl. Phys. 40, 1368 (1969).

[11] M. A. Kahn, J. Phys. F 9, 457 (1979).

[12] C. Koenig, J. Phys. F 19, 1123 (1982).

[13] H. Hasegawa, J. Magn. Magn. Mater. 66, 175 (1987).

[14] V. L. Moruzzi, Phys. Rev. B 41, 6939 (1990).

[15] The type-I and type-II antiferromagnetic classifications used here for the simple-cubic lattice of iron atoms are made by analogy with the classification for bcc lattices given by R. S. Tebble and D. J. Craik, Magnetic Materials (Wiley Interscience, New York, 1969), p. 23.

[16] A. R. Williams, J. Kübler, and C. D. Gelatt, Jr., Phys. Rev. B 19, 6094 (1979).

[17] U. von Barth and L. Hedin, J. Phys. C 5, 1692 (1972); J. F. Janak, Solid State Commun. 25, 53 (1978).

[18] Cs. Hargitai, Phys. Lett. 17, 178 (1965).

[19] G. Shirane, R. Nathans, and C. W. Chen, Phys. Rev. 134, A1547 (1964).

[20] V. L. Moruzzi, J. F. Janak, and K. Schwarz, Phys. Rev. B 37, 790 (1988).

[21] V. L. Moruzzi, Phys. Rev. Lett. 57, 2211 (1986).

[22] V. L. Moruzzi, J. F. Janak, and A. R. Williams, Calculated

Electronic Properties of Metals (Pergamon, New York, 1978), p. 168.

[23]Liang-Yao Chen and David W. Lynch, Phys. Rev. B **37**, 10 503 (1988).

[24]V. L. Moruzzi, Physica B **161**, 99 (1989).

[25]V. L. Moruzzi and P. M. Marcus, Phys. Rev. B **45**, 2934 (1992).

FIG. 1. Spin configurations for type-I and type-II antifer-romagnetism for the basic CsCl unit cell for FeRh. Shaded and open spheres represent rhodium and iron atoms. Configuration (II) with no spin on the rhodium atom is experimentally observed. In the ferromagnetic state, all iron and rhodium spins are parallel.
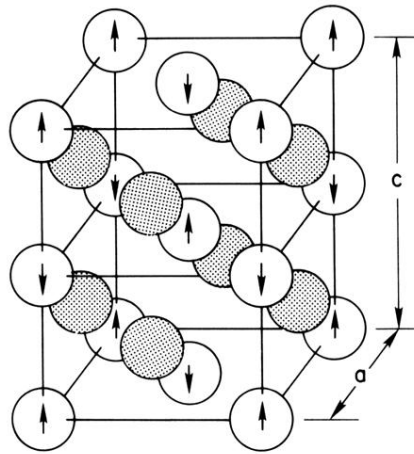
FIG. 2. Magnetic unit cell used to study both antiferromagnetic and ferromagnetic states in FeRh. Shaded and open spheres represent rhodium and iron atoms, respectively. Arrows indicate the antiferromagnetic iron spin configuration. In the antiferromagnetic state, the rhodium atoms have no local moments. In the ferromagnetic state, all iron spins and rhodium spins are parallel.